

# Beampattern Synthesis for Linear and Planar Arrays With Antenna Selection by Convex Optimization

Siew Eng Nai, *Graduate Student Member, IEEE*, Wee Ser, *Senior Member, IEEE*, Zhu Liang Yu, *Member, IEEE*, and Huawei Chen, *Member, IEEE*

**Abstract**—A convex optimization based beampattern synthesis method with antenna selection is proposed for linear and planar arrays. Conjugate symmetric beamforming weights are used so that the upper and non-convex lower bound constraints on the beampattern can be convex. Thus, a mainlobe of an arbitrary beamwidth and response ripple can be obtained. This method can achieve completely arbitrary sidelobe levels. By minimizing a re-weighted objective function based on the magnitudes of the elements in the beamforming weight vector iteratively, the proposed method selects certain antennas in an array to satisfy the prescribed beampattern specifications precisely. Interestingly, a sparse array with fewer antennas (compared to other methods) is produced. This method can design non-uniformly spaced arrays with inter-element spacings larger than one half-wavelength, without the appearance of grating lobes in the resulting beampattern. Simulations are shown using arrays of up to a few hundred antennas to illustrate the practicality of the proposed method.

**Index Terms**—Array signal processing, directive antennas, linear arrays, mutual coupling, planar arrays, robustness.

## I. INTRODUCTION

**I**N real array processing scenarios, the actual direction-of-arrival of the desired signal is usually unknown or estimated with some errors [1]–[4]. Thus, it becomes important to design a mainlobe with both controllable beamwidth and response

ripple to provide robustness. This requires constraints to simultaneously control the upper and lower bounds of the mainlobe. However, the lower bound constraint is non-convex [2], [5]. To overcome this, [4]–[7] use the array weight autocorrelation sequence to transform the non-convex constraint into a convex one but this approach is limited to uniformly spaced arrays.

It is desirable to be able to design completely arbitrary sidelobe levels. If there are prior information about the approximate locations of strong interferences, broadened deepened nulls (of specified widths and rejection levels) can be incorporated into the beampattern design to eliminate the degradation they introduce to the array system [4]. Classical synthesis methods of Dolph [8], Tseng and Cheng [9], and Kim and Elliott [10] cannot design completely arbitrary sidelobe levels. The method of Woodward and Lawson [11] can achieve an arbitrary beampattern. However, [8]–[11] are all restricted to uniformly spaced arrays. Though applicable to non-uniformly spaced arrays, the methods of [12], [13] cannot control the beampattern precisely according to the required specifications.

For beampattern synthesis, it is economical to use as few antennas as possible to minimize the weight, cost, and complexity of the array system. The reviewed methods did not consider decreasing the number of antennas needed. Hence, this paper proposes a convex optimization based beampattern synthesis method with antenna selection for linear and planar arrays. Conjugate symmetric beamforming weights are used so that the non-convex lower bound constraint on the beampattern can be affine (thus convex). The resulting upper bound constraint on the beampattern is also affine. This facilitates the design of a mainlobe with controllable beamwidth and response ripple. Arbitrary sidelobe levels can also be designed. The proposed method minimizes a re-weighted objective function based on the magnitudes of the elements in the beamforming weight vector iteratively to suppress its small elements to zero. A zero element in the beamforming weight vector implies that the corresponding antenna is redundant. This results in a more efficient beampattern requiring fewer antennas that satisfies the same specifications achieved by a non-sparse array. The proposed method can be used to design non-uniformly spaced arrays (with inter-element spacings larger than one half-wavelength) for an arbitrary beampattern precisely without suffering from grating lobes. Unlike [8], the proposed method also applies directly when the antennas have the same directive element pattern by factoring the element pattern into the proposed constraints. In this paper, the polarization of the array antennas is considered to match that of the impinging wave so as to extract the maximum power from it [14].

Manuscript received August 03, 2009; revised January 08, 2010; accepted May 14, 2010. Date of publication September 23, 2010; date of current version November 30, 2010. The work of S. E. Nai was supported by the Agency for Science, Technology and Research (A\*STAR), Singapore. The work of Z. L. Yu was supported in part by the National Natural Science Foundation of China under Grant 60802068, Guangdong Natural Science Foundation under Grant 8451064101000498, the Program for New Century Excellent Talents in University under Grant NCET-10-0370, and in part by the Fundamental Research Funds for the Central Universities, SCUT under Grant 2009ZZ0055. The work of H. Chen was supported in part by the National Natural Science Foundation of China under Grant 61001150, the Natural Science Foundation of Jiangsu Province, China, under Grant BK2010495, and in part by the Research Foundation of Nanjing University of Aeronautics and Astronautics (NUAA).

S. E. Nai is with the School of Electrical and Electronic Engineering, Nanyang Technological University, Singapore 639798, Singapore and also with the Institute for Infocomm Research, A\*STAR, Singapore 138632, Singapore (e-mail: senai@i2r.a-star.edu.sg).

W. Ser is with the Centre for Signal Processing, School of Electrical and Electronic Engineering, Nanyang Technological University, Singapore 639798, Singapore (e-mail: ewser@ntu.edu.sg).

Z. L. Yu is with the College of Automation Science and Engineering, South China University of Technology, Guangzhou, China (e-mail: zhuliang.yu@ieee.org).

H. Chen is with the College of Information Science and Technology, Nanjing University of Aeronautics and Astronautics, Nanjing, China (e-mail: hwchen@nuaa.edu.cn).

Color versions of one or more of the figures in this paper are available online at <http://ieeexplore.ieee.org>.

Digital Object Identifier 10.1109/TAP.2010.2078446

Due to mutual coupling and array imperfections, the actual array manifold may differ from the presumed one. Thus, the synthesized beam pattern by the proposed method may violate the specifications. Robust beam pattern constraints are derived for the antenna selection method based on the uncertainty set of the actual array manifold and worst-case performance optimization. Simulation results show that the resulting beam patterns are robust against mutual coupling effects and array imperfections while satisfying specifications wholly without increasing the number of selected antennas. The proposed method can help select the antennas in an array for application fields, e.g., radar, satellite and mobile communications [15]. The antenna selection method with robust constraints is a (convex) second-order cone program (SOCP) that can be solved by the interior point method (IPM)<sup>1</sup> efficiently in polynomial-time with open-source solvers,<sup>2</sup> e.g., [16].

## II. DATA MODEL

A rectangular planar array is considered with  $N$  and  $M$  isotropic antennas in the  $x$  and  $y$  directions, respectively. The inter-element spacings are  $d_x$  and  $d_y$  in the  $x$  and  $y$  directions, respectively. A linear array can be easily derived. A plane wave of  $\lambda$  wavelength impinges on the array in a  $(\theta, \phi)$  direction where  $\theta$  and  $\phi$  denote the azimuth and polar angles, respectively. With direction cosines  $u_x = \sin \phi \cos \theta$  and  $u_y = \sin \phi \sin \theta$  [15], the array beam pattern is defined as

$$G(u_x, u_y) = \sum_{n=1}^N \sum_{m=1}^M w_{n,m} e^{j \frac{2\pi}{\lambda} n d_x u_x + j \frac{2\pi}{\lambda} m d_y u_y} \quad (1)$$

with complex array weights  $w_{n,m} \in \mathbb{C}^{NM}$  for  $n = 1, \dots, N$  and  $m = 1, \dots, M$ . A typical mainlobe design constraint is

$$l \leq |G(u_x, u_y)| \leq u, \quad u_x, u_y \in [-1, 1] \quad (2)$$

where  $|\cdot|$  is the absolute operator,  $l$  and  $u$  are constants denoting the lower and upper magnitude response bounds, respectively. Such a constraint offers flexibility in controlling the mainlobe beamwidth and response ripple. Although (2) is intuitive, it is not widely employed in beam pattern synthesis applications as the lower bound constraint  $l \leq |G(u_x, u_y)|$  is non-linear, non-convex, and thus, NP-hard<sup>3</sup> to solve.

## III. PROPOSED BEAMPATTERN CONSTRAINTS

The aim here is to develop convex lower and upper magnitude response constraints on the beam pattern. To this end, conjugate symmetric beamforming weights are proposed;  $w_{i,j} = w_{N-i+1, M-j+1}^*$ , i.e.,  $w_{1,1} = w_{N,M}^*$ ,  $w_{1,2} = w_{N,M-1}^*$ , and

<sup>1</sup>IPMs do not suffer from algorithmic initialization and stepsize selection problems unlike the traditional gradient-based optimization techniques [4].

<sup>2</sup>In the case of inappropriate beam pattern specifications, the solver issues a certificate of infeasibility to inform the system designer.

<sup>3</sup>NP-hard (non-deterministic polynomial-time)-hard problems are “extremely difficult problems with no known polynomial-time solutions” [2].

so on where  $(\cdot)^*$  is the complex conjugate operator. Thus, the beam pattern in (1) can be written as

$$\begin{aligned} G(u_x, u_y) &= e^{j \frac{2\pi}{\lambda} (\frac{N+1}{2}) d_x u_x + j \frac{2\pi}{\lambda} (\frac{M+1}{2}) d_y u_y} \\ &\times \left[ w_{1,1} e^{-j \frac{2\pi}{\lambda} (\frac{N-1}{2}) d_x u_x - j \frac{2\pi}{\lambda} (\frac{M-1}{2}) d_y u_y} \right. \\ &+ w_{1,2} e^{-j \frac{2\pi}{\lambda} (\frac{N-1}{2}) d_x u_x - j \frac{2\pi}{\lambda} (\frac{M-1}{2}-1) d_y u_y} + \dots \\ &+ w_{(\frac{N-1}{2}+1), (\frac{M-1}{2}+1)} + \dots \\ &+ w_{1,2}^* e^{j \frac{2\pi}{\lambda} (\frac{N-1}{2}) d_x u_x + j \frac{2\pi}{\lambda} (\frac{M-1}{2}-1) d_y u_y} \\ &\left. + w_{1,1}^* e^{j \frac{2\pi}{\lambda} (\frac{N-1}{2}) d_x u_x + j \frac{2\pi}{\lambda} (\frac{M-1}{2}) d_y u_y} \right]. \quad (3) \end{aligned}$$

The magnitude response  $|G(u_x, u_y)|$  is then expressed as

$$\begin{aligned} |G(u_x, u_y)| &= 2\text{Re} \left\{ w_{1,1} e^{-j \frac{2\pi}{\lambda} (\frac{N-1}{2}) d_x u_x - j \frac{2\pi}{\lambda} (\frac{M-1}{2}) d_y u_y} \right. \\ &+ w_{1,2} e^{-j \frac{2\pi}{\lambda} (\frac{N-1}{2}) d_x u_x - j \frac{2\pi}{\lambda} (\frac{M-1}{2}-1) d_y u_y} + \dots \\ &\left. + w_{(\frac{N-1}{2}+1), (\frac{M-1}{2}+1)} \right\} \quad (4) \end{aligned}$$

where  $\text{Re}\{\cdot\}$  is a real operator. Odd  $N$  and  $M$  are assumed. The extension to even  $N$  and  $M$  follows similarly. With conjugate symmetric beamforming weights, the imaginary parts of the terms in the square brackets of (3) cancel out. Thus,  $|G(u_x, u_y)|$  in (4) is a real function, any lower or upper bound on it is affine. The expression (4) is rewritten as  $|G(u_x, u_y)| = \mathbf{s}^T(u_x, u_y) \mathbf{w}$  where  $(\cdot)^T$  is a transpose operator and the non-convex constraint (2) is equivalent to

$$l \leq \mathbf{s}^T(u_x, u_y) \mathbf{w} \leq u \quad (5)$$

where

$$\begin{aligned} \mathbf{s}(u_x, u_y) &= \begin{bmatrix} e^{-j \frac{2\pi}{\lambda} (\frac{N-1}{2}) d_x u_x - j \frac{2\pi}{\lambda} (\frac{M-1}{2}) d_y u_y} \\ e^{-j \frac{2\pi}{\lambda} (\frac{N-1}{2}) d_x u_x - j \frac{2\pi}{\lambda} (\frac{M-1}{2}-1) d_y u_y} & \dots & 1 & \dots \\ e^{j \frac{2\pi}{\lambda} (\frac{N-1}{2}) d_x u_x + j \frac{2\pi}{\lambda} (\frac{M-1}{2}-1) d_y u_y} \\ e^{j \frac{2\pi}{\lambda} (\frac{N-1}{2}) d_x u_x + j \frac{2\pi}{\lambda} (\frac{M-1}{2}) d_y u_y} \end{bmatrix}^T \end{aligned}$$

is the array manifold of a rectangular planar array. For each  $(u_x, u_y)$ , the constraint (5) is a pair of linear inequalities in  $\mathbf{w}$  and thus, convex over  $\mathbf{w}$ .

The constraint (5) is used to provide direct control over the mainlobe region ( $U_{ML}$ ) in (6b), and modified for the sidelobe ( $U_{SL}$ ) and null ( $U_N$ ) regions, respectively in (6c)–(6d) as

$$\min_{\mathbf{w}} \quad \tau \quad (6a)$$

$$\text{s.t.} \quad l \leq \mathbf{s}^T(u_x, u_y) \mathbf{w} \leq u, \{u_x, u_y\} \in U_{ML} \quad (6b)$$

$$\mathbf{s}^T(u_x, u_y) \mathbf{w} \leq \tau, \{u_x, u_y\} \in U_{SL} \quad (6c)$$

$$\mathbf{s}^T(u_x, u_y) \mathbf{w} \leq \tau_n, \{u_x, u_y\} \in U_N. \quad (6d)$$

Though the objective of this paper is to develop an antenna selection synthesis method, for completeness, an important syn-

thesis aim (sidelobe level minimization) is briefly shown in (6). The problem (6) minimizes  $\tau$  which is the magnitude response of  $U_{SL}$ , although other beampattern parameters may be minimized.  $\tau_n$  is a user-specified parameter which is the magnitude response of  $U_N$ . The problem (6) is a (convex) linear program (LP) with affine objective function and constraints. Given that (6) is an LP,<sup>4</sup> it can be solved globally by the IPM.<sup>5</sup> The solution  $\tau$  thus obtained is the best that can be achieved, even by other methods with the same constraints.

The designed constraints (6b) and (6c)–(6d) can generate completely arbitrarily shaped mainlobe and arbitrary sidelobe levels with specified magnitude responses (precisely), respectively. This capability is lacking in the methods of [8]–[10]. For example, to obtain a diamond-shaped or circular-shaped mainlobe, the mainlobe region in (6b) is defined as  $\{(u_x, u_y) \mid |u_x| + |u_y| \leq u_p\} \in U_{ML}$  or  $\{(u_x, u_y) \mid u_x^2 + u_y^2 \leq u_p^2\} \in U_{ML}$ , respectively where  $u_p$  is a specified constant.

#### IV. PROPOSED BEAMPATTERN SYNTHESIS METHOD WITH ANTENNA SELECTION

This section aims to find an array with as few antennas as possible to achieve the constraints (6b)–(6d).

##### A. Problem Development

Our problem of interest is related to finding the sparsest  $\mathbf{w}$

$$\min_{\mathbf{w}} \quad \|\mathbf{w}\|_0 \quad (7a)$$

$$\text{s.t.} \quad l \leq \mathbf{s}^T(u_x, u_y)\mathbf{w} \leq u, \{u_x, u_y\} \in U_{ML} \quad (7b)$$

$$\mathbf{s}^T(u_x, u_y)\mathbf{w} \leq \tau, \{u_x, u_y\} \in U_{SL} \quad (7c)$$

$$\mathbf{s}^T(u_x, u_y)\mathbf{w} \leq \tau_n, \{u_x, u_y\} \in U_N \quad (7d)$$

where the  $l_0$ -quasi norm  $\|\cdot\|_0$  is the count of the number of non-zero elements of its argument.<sup>6</sup> For (7)–(9),  $\tau$  is a user-specified term. Though (7b)–(7d) are convex, (7) is a NP-hard combinatorial optimization problem due to the non-convex objective function. To find the globally optimal solution, an exhaustive combinatorial search through  $2^{NM/2}$  sparsity patterns of  $\mathbf{w}$  is required because each  $w_k$  can either take on values of zero or non-zero. For each of these combinations, a convex problem results but the exhaustive search is easily intractable for a modest-sized array.

To circumvent the intractable problem (7), a good approach is to approximate or relax it in a convex manner by solving

$$\min_{\mathbf{w}} \quad \|\mathbf{w}\|_1 \quad (8a)$$

$$\text{s.t.} \quad l \leq \mathbf{s}^T(u_x, u_y)\mathbf{w} \leq u, \{u_x, u_y\} \in U_{ML} \quad (8b)$$

$$\mathbf{s}^T(u_x, u_y)\mathbf{w} \leq \tau, \{u_x, u_y\} \in U_{SL} \quad (8c)$$

$$\mathbf{s}^T(u_x, u_y)\mathbf{w} \leq \tau_n, \{u_x, u_y\} \in U_N \quad (8d)$$

<sup>4</sup>An important property of convex problems is that any local optimum is the global optimum [17].

<sup>5</sup>IPM has the advantage of polynomial complexity over the simplex algorithm in solving LPs [18].

<sup>6</sup> $l_0$ -quasi norm is not a valid norm as it violates the triangle inequality.

where  $\|\mathbf{x}\|_1 = \sum_{k=1}^{NM} |x_k|$  is known as the  $l_1$ -norm. Indeed, the  $l_1$ -norm is the closest convex function to  $l_0$ -quasi norm and the  $l_1$ -norm is known to produce sparse solutions for many applications<sup>7</sup>. The problem (8) is a SOCP.

To further increase the sparsity of  $\mathbf{w}$ , the algorithm in [20], [21] is modified for our beampattern synthesis problem.<sup>8</sup> In the proposed antenna selection method (9), a re-weighted  $l_1$ -norm of the vector  $\mathbf{w}$  is minimized at each step as

$$\min_{\mathbf{w}^i} \quad \sum_{k=1}^{NM} \varphi(w_k^{i-1})|w_k^i| \quad (9a)$$

$$\text{s.t.} \quad l \leq \mathbf{s}^T(u_x, u_y)\mathbf{w}^i \leq u, \{u_x, u_y\} \in U_{ML} \quad (9b)$$

$$\mathbf{s}^T(u_x, u_y)\mathbf{w}^i \leq \tau, \{u_x, u_y\} \in U_{SL} \quad (9c)$$

$$\mathbf{s}^T(u_x, u_y)\mathbf{w}^i \leq \tau_n, \{u_x, u_y\} \in U_N \quad (9d)$$

where the weightings  $\varphi(w_k^{i-1}) = 1/(|w_k^{i-1}| + \delta)$  are assigned to each of the elements of  $\mathbf{w}^i$  ( $\mathbf{w}$  at  $i$ th iteration). The threshold  $\delta > 0$  provides numerical stability and helps determine if a particular  $w_k$  should be considered zero.  $\delta$  is small and fixed during the iterations. In the first iteration ( $i = 1$ ), the weightings  $\varphi(w_k^0)$  can be initialized to all ones and the resulting objective function (9a) becomes  $\sum_{k=1}^{NM} |w_k| = \|\mathbf{w}\|_1$ . Thus, the equivalent problem to solve in the first iteration is (8) which is a good initializer for (9).

With the obtained  $w_k^i$ , those of small magnitudes are given larger weightings  $1/(|w_k^i| + \delta)$  in the next iteration and vice versa. At each iteration, a positive weighted sum of the magnitudes of the elements in  $\mathbf{w}$  is minimized to produce a new  $\mathbf{w}$  hence the proposed method (9) is still a SOCP. The iterative procedure repeats until the maximum number of iterations is reached. This value can be readily obtained by simple trial-and-error during the design process. By extensive simulations, we found that it is suitable to set as 20. The result is that the small entries in  $\mathbf{w}$  are suppressed to zero, as far as the constraints allow and thus, yielding a sparse  $\mathbf{w}$ .

The proposed method (9) can help reduce the Dynamic Range Ratio (DRR) of  $\mathbf{w}$  to ease the design and implementation of the feed networks. A direct way to lower the DRR may be to eliminate antennas with small weights but the resulting beampattern may violate the specifications. Instead,  $\mathbf{w}$  is continually adjusted at each iteration of the proposed method (9) according to the magnitudes of its elements (to increase its sparsity) while satisfying the specifications precisely.

##### B. Algorithm Summary and Remarks

The proposed antenna selection method (9) is summarized.

- 1) In the first iteration ( $i = 1$ ), initialize  $\varphi(w_k^{i-1}) = \varphi(w_k^0) = 1$  for all  $k$ . Therefore, the equivalent problem to solve is (8).

<sup>7</sup>Theoretical analysis on the sparsity-promoting properties of the  $l_1$ -norm can be found in [19] and the references therein.

<sup>8</sup>The algorithm is used for sparse signal recovery [20] and for portfolio optimization with real-valued variables [21]. In this paper, the algorithm is modified for a new problem for beampattern synthesis applications where the optimized beamforming weight vector is complex-valued.

- 2) For subsequent iterations ( $i > 1$ ), with a fixed  $\delta = 10^{-5}$  (this choice is discussed in Section VI) and  $w_k^{i-1}$ , set  $\varphi(w_k^{i-1}) = 1/(|w_k^{i-1}| + \delta)$  and solve (9).
- 3) Repeat step (2) until the maximum number of iterations = 20 is reached.

Some remarks on the proposed methods (6) and (9) are:

- The antenna selection method (9) can be used to switch off antennas in existing arrays for different beam pattern designs. Next, compared to uniformly spaced arrays, an array with the same number but arbitrarily spaced antennas has more degrees of freedom, suggesting that the design of non-uniformly spaced arrays can reduce the number of antennas required [22]. Thus, (9) can be used to design such arrays for prescribed beam pattern specifications before the actual array is mounted.
- While the antenna selection method (9) is not guaranteed to reach a globally optimal solution<sup>9</sup> for (7), it converges very quickly with few iterations as observed in the simulations in Section VI.
- Unlike [8], the proposed methods (6) and (9) can still be applied directly when all the antennas have the same directive pattern  $p(u_x, u_y)$  by modifying the proposed constraint as  $l \leq p(u_x, u_y)[\mathbf{s}^T(u_x, u_y)\mathbf{w}] \leq u$ .
- The polarization of the array antennas is considered to match that of the impinging wave so as to extract the maximum power from it [14]. Equations (6) and (9) are not restricted to arrays with the same number of antennas in both x and y directions ( $N \neq M$ ), unlike [9]. The inter-element spacings can be different ( $d_x \neq d_y$ ).

## V. ROBUSTNESS ISSUES

Due to mutual coupling or array imperfections, the actual array manifold  $\tilde{\mathbf{s}}(u_x, u_y)$  can be unknown and it can differ from the ideal presumed one  $\mathbf{s}(u_x, u_y)$ . Thus, the synthesized beam pattern by (6) or (9) may violate the specifications. To improve the robustness of the proposed methods (6) and (9) against various undesirable effects, the worst-case performance optimization technique [2], [17] is applied. To illustrate, mutual coupling effects are considered by means of a coupling matrix  $\mathbf{C}$ . The actual array manifold is  $\tilde{\mathbf{s}}(u_x, u_y) = \mathbf{C}\mathbf{s}(u_x, u_y)$  which belongs to an uncertainty set modelled as

$$\Upsilon(\eta) = \{\tilde{\mathbf{s}}(u_x, u_y) | \tilde{\mathbf{s}}(u_x, u_y) = \mathbf{s}(u_x, u_y) + \mathbf{e}(u_x, u_y)\} \quad (10)$$

where the complex error  $\mathbf{e}(u_x, u_y)$  is norm-bounded by a known constant  $\|\mathbf{e}(u_x, u_y)\| \leq \eta(u_x, u_y) = \eta$  (for simplicity). The previous proposed mainlobe constraint is rewritten as

$$l \leq \min |\tilde{\mathbf{s}}^T(u_x, u_y)\mathbf{w}| \leq \max |\tilde{\mathbf{s}}^T(u_x, u_y)\mathbf{w}| \leq u. \quad (11)$$

Applying the triangle and Cauchy-Schwarz inequalities yields

$$|\tilde{\mathbf{s}}^T(u_x, u_y)\mathbf{w}| = |\mathbf{s}^T(u_x, u_y)\mathbf{w} + \mathbf{e}^T(u_x, u_y)\mathbf{w}| \quad (12)$$

$$\geq |\mathbf{s}^T(u_x, u_y)\mathbf{w}| - |\mathbf{e}^T(u_x, u_y)\mathbf{w}| \quad (13)$$

$$\geq \mathbf{s}^T(u_x, u_y)\mathbf{w} - \eta\|\mathbf{w}\| \quad (14)$$

<sup>9</sup>A combinatorial search through  $2^{NM/2}$  sparsity patterns of  $\mathbf{w}$  to find the globally optimal solution is intractable for the size of arrays considered in this paper.

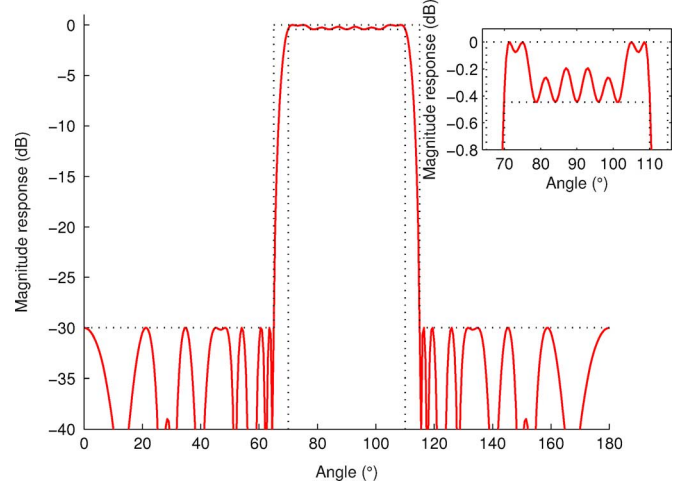


Fig. 1. Beam pattern achieved by the proposed antenna selection method (9) using 31 selected antennas in a non-uniformly spaced linear array. A close-up view of the mainlobe is shown in the inset. The beam pattern has to be lower than the outer dotted lines and higher than the inner dotted lines.

where  $\mathbf{s}^T(u_x, u_y)\mathbf{w} > \eta\|\mathbf{w}\|$ , equality holds with  $\mathbf{e}(u_x, u_y) = -\eta(\mathbf{w}/\|\mathbf{w}\|)e^{j\psi}$  and  $\psi = \angle\{\mathbf{s}^T(u_x, u_y)\mathbf{w}\} = 0$  as  $\mathbf{s}^T(u_x, u_y)\mathbf{w}$  is real. Thus,  $\min |\tilde{\mathbf{s}}^T(u_x, u_y)\mathbf{w}| = \mathbf{s}^T(u_x, u_y)\mathbf{w} - \eta\|\mathbf{w}\|$ . Also, similarly

$$|\tilde{\mathbf{s}}^T(u_x, u_y)\mathbf{w}| \leq \mathbf{s}^T(u_x, u_y)\mathbf{w} + |\mathbf{e}^T(u_x, u_y)\mathbf{w}| \quad (15)$$

$$\leq \mathbf{s}^T(u_x, u_y)\mathbf{w} + \eta\|\mathbf{w}\| \quad (16)$$

where equality holds with  $\mathbf{e}(u_x, u_y) = \eta(\mathbf{w}/\|\mathbf{w}\|)$ . As  $\max |\tilde{\mathbf{s}}^T(u_x, u_y)\mathbf{w}| = \mathbf{s}^T(u_x, u_y)\mathbf{w} + \eta\|\mathbf{w}\|$ , (11) becomes

$$\mathbf{s}^T(u_x, u_y)\mathbf{w} - \eta\|\mathbf{w}\| \geq l, \{u_x, u_y\} \in U_{\text{ML}} \quad (17a)$$

$$\mathbf{s}^T(u_x, u_y)\mathbf{w} + \eta\|\mathbf{w}\| \leq u, \{u_x, u_y\} \in U_{\text{ML}}. \quad (17b)$$

Equation (17b) can be extended to  $U_{\text{SL}}$  and  $U_{\text{N}}$ . When these robust second-order-cone (SOC) constraints in (17) are used in (6) and (9), the resulting (6) and (9) are SOCPs.

## VI. SIMULATION RESULTS

This section tests the proposed synthesis method (6) and antenna selection method (9). For (9), the maximum number of iterations is 20 and  $\delta = 10^{-5}$  (this choice is discussed later). The antennas used are isotropic unless stated otherwise.

### A. Linear Arrays

In the first example, the antenna selection method (9) is used on a non-uniformly spaced 41-antenna array from [13], [23]. Antenna positions are given in [23]. A two-step least-squares approach is developed in [13] and the same beam pattern specifications are used here. The mainlobe beamwidth and response ripple  $r_{\text{dB}}$  are  $40^\circ$  and  $0.4455$  dB, respectively. The sidelobe region is  $[0^\circ, 65^\circ] \cup [115^\circ, 180^\circ]$  and  $\tau = -30$  dB. Specifications are shown in dotted lines. In the first iteration, a  $l_1$ -norm version of (9) is solved and the solution is 39 antennas. The final solution found by (9) is 31 antennas (obtained at the 4th iteration) and the resulting beam pattern is shown in Fig. 1 Compared to [13], 10 antennas are saved.

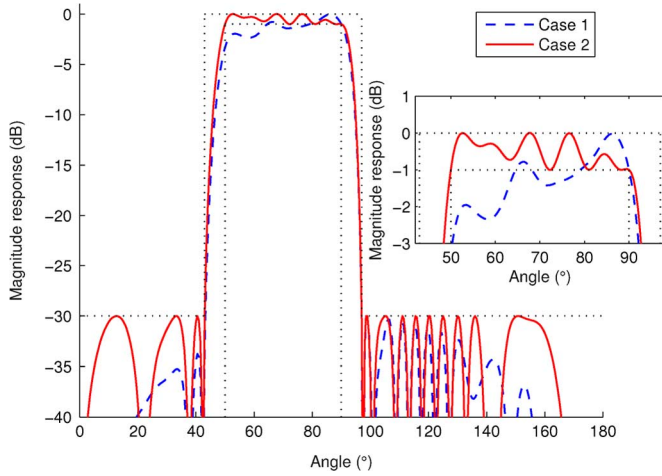


Fig. 2. Beam patterns achieved by the proposed antenna selection method (9) in Case 1 and Case 2, without and with antenna element pattern  $p(\theta) = \sin(\theta)$  consideration, respectively. 27 and 25 antennas are selected in a non-uniformly spaced linear array for Case 1 and Case 2, respectively. A close-up view of the mainlobe is shown in the inset. The beam pattern has to be lower than the outer dotted lines and higher than the inner dotted lines.

In the second example, the antenna selection method (9) is used on the same non-uniformly spaced array as the first example but with directive antennas of element pattern  $p(\theta) = \sin(\theta)$ , e.g., short dipoles located on and aligned with the x-axis. The same specifications are used except that  $r_{dB} = 1$  dB and the sidelobe region is  $[0^\circ, 43^\circ] \cup [97^\circ, 180^\circ]$ . Case 1 ignores  $p(\theta)$  and 27 antennas are selected by (9) (obtained at the 3rd iteration). Case 2 considers  $p(\theta)$  in the optimization and only 25 antennas are selected by (9) (obtained at the 6th iteration). Fig. 2 shows that the beam pattern in Case 1 (plotted in dashed line) violates the mainlobe specifications whereas the beam pattern in Case 2 (plotted in solid line) satisfies all the specifications.

In the third example, the same 41-antenna array and specifications as the second example are used except that the sidelobe region is  $[0^\circ, 63^\circ] \cup [117^\circ, 180^\circ]$ . All the antennas are assumed to have the same element pattern  $p(\theta) = \sin(\theta)$ . In Case 3, the antenna selection method chooses 19 antennas (obtained at the 2nd iteration) to achieve the specifications. However, the element pattern of the 20th antenna (weight magnitude  $> \delta = 10^{-5}$ ) is  $\sin^{1.2}(\theta)$ . Thus, the resulting beam pattern (plotted in dashed line) for Case 3 in Fig. 3 violates the specifications. In Case 4, the proposed robust constraints for the mainlobe and sidelobe regions are used with the antenna selection method where  $\eta_m$  for mainlobe and sidelobe regions are  $\eta_m = 0.001$  and  $\eta_s = 0.007$ , respectively. The resulting beam pattern (plotted in solid line) in Fig. 3 satisfies all the specifications using the same 19 antennas (obtained at the 3rd iteration). The antenna selection method (9) with the robust constraints is found to be insensitive to  $\eta_m$  and  $\eta_s$  in  $0.001 \leq \eta_m \leq 0.023$  and  $0.0065 \leq \eta_s \leq 0.007$ , respectively.

In the fourth example, a  $\lambda/2$  spaced uniform array of thin half-wavelength dipoles is used to consider mutual coupling effects. They are located along the x-axis and aligned with the z-axis. Accordingly, the coupling matrix  $\mathbf{C}$  is calculated by the induced electromotive force approach ([14], Ch. 8). The same specifications in the third example are used. First, mutual coupling is ignored. The synthesis method (6) is tested and

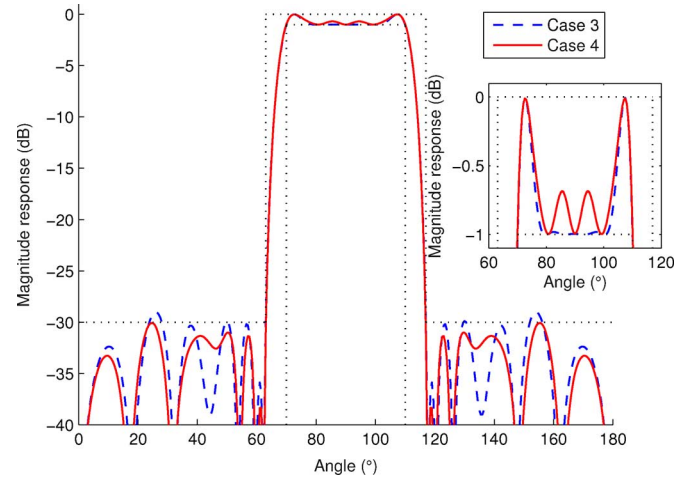


Fig. 3. Beam patterns achieved by the proposed antenna selection method (9) using 19 antennas, without and with robust constraints in Case 3 and Case 4, respectively. The 20th antenna has a different element pattern from the rest. A close-up view of the mainlobe is shown in the inset. The beam pattern has to be lower than the outer dotted lines and higher than the inner dotted lines.

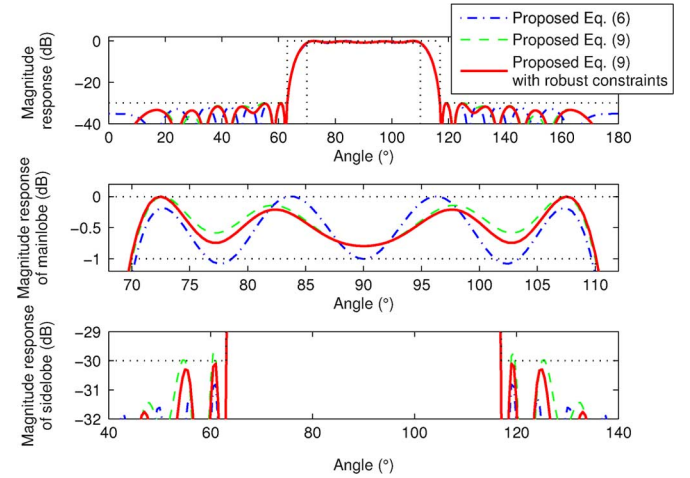


Fig. 4. Top: Beam patterns achieved by the proposed synthesis method (6) with 23 selected antennas, proposed antenna selection method (9) without and with robust constraints using 18 selected antennas, in the presence of mutual coupling. Middle: A close-up view of the mainlobe. Bottom: A close-up view of the sidelobe. The beam pattern has to be lower than the outer dotted lines and higher than the inner dotted lines.

at least 23 antennas are needed to achieve the specifications. The resulting beam pattern in the presence of mutual coupling is plotted in dotted-dashed line in Fig. 4 which violates the mainlobe specifications. Again, mutual coupling is ignored and the antenna selection method (9) selects only 18 antennas (obtained at the 2nd iteration) out of a 24-antenna uniform array to achieve the same specifications. The resulting beam pattern in the presence of mutual coupling is plotted in the dashed line in Fig. 4 which violates the specifications. To compensate for mutual coupling effects, robust constraints for the mainlobe and sidelobe regions are used with the antenna selection method (9) where  $\eta_m = 0.001$  and  $\eta_s = 0.003$ . The resulting beam pattern (plotted in solid line) in Fig. 4 satisfies the specifications in the presence of mutual coupling with the same 18 antennas (obtained at the 2nd iteration). The antenna selection method (9) with the robust constraints is found to be insensitive to  $\eta_m$



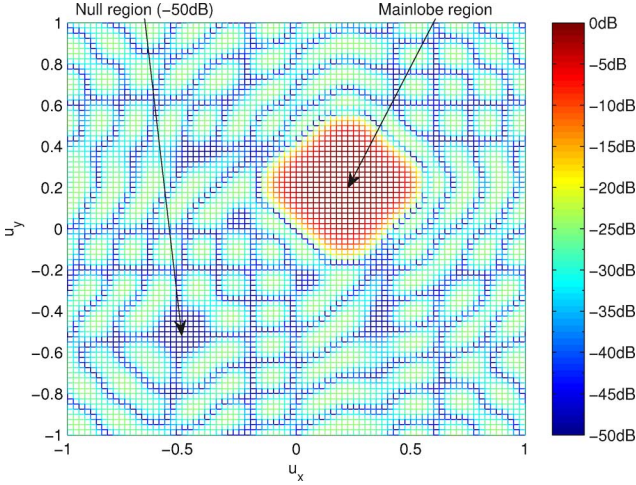


Fig. 5. Beam pattern with diamond-shaped mainlobe, controlled sidelobe level, and circular-shaped null achieved by the proposed synthesis method (6) with a  $14 \times 14$  array.

and  $\eta_s$  in  $0.0001 \leq \eta_m \leq 0.001$  and  $0.003 \leq \eta_s \leq 0.006$ , respectively. The consideration for  $p(\theta)$  and compensation for the distortions can be extended similarly to planar arrays.

#### B. Planar Arrays

Next,  $\lambda/2$  spaced rectangular planar arrays are considered and beam patterns are plotted in  $u_x - u_y$  axes ([15], Ch. 4). In the fifth example, a beam pattern with a diamond-shaped mainlobe, controlled sidelobe level, and circular-shaped null region is designed by the synthesis method (6). A  $14 \times 14$  array is used. The mainlobe is  $|u_x - 0.2| + |u_y - 0.2| \leq 0.2$  with  $r_{dB} = 1$  dB. The sidelobe region is  $|u_x - 0.2| + |u_y - 0.2| \geq 0.4$ . The null region is  $(u_x + 0.5)^2 + (u_y + 0.5)^2 \leq 0.1^2$  with  $\tau_n = -50$  dB. The synthesized beam pattern in Fig. 5 meets all the requirements (including arbitrary sidelobe levels) and the minimal sidelobe level achieved is  $\tau = -24.30$  dB.

In the sixth example, the synthesis method (6) is used to design a circular-shaped mainlobe with controlled sidelobe level. A  $11 \times 11$  array is used. The total number of antennas is 121. The mainlobe region is  $u_x^2 + u_y^2 \leq 0.2^2$  with  $r_{dB} = 1$  dB. The sidelobe region is  $u_x^2 + u_y^2 \geq 0.4^2$ . The minimal sidelobe level achieved is  $\tau = -25.85$  dB. For brevity, the synthesized beam patterns in the sixth and seventh examples are not shown. A final representative beam pattern (with same specifications) is shown in the eighth example by Fig. 8. All the 121 antennas here are used (with magnitudes  $> \delta = 10^{-5}$ ). Element magnitudes in  $\mathbf{w} \leq 10^{-5}$  are considered zero, for a fair comparison with the antenna selection method (9).

In the seventh example, the antenna selection method (9) is used on the same  $11 \times 11$  array to produce a sparse one which satisfies the same specifications in the sixth example. In the first iteration, a  $l_1$ -norm version of (9) is solved and the solution is 105 antennas. The final solution found by (9) is 85 antennas (obtained at the 2nd iteration). The  $\lambda/2$  spaced  $11 \times 11$  array with the selected antennas is shown in Fig. 6, accounting for 70% of those in the original array. The selected antennas are indicated with circles while the unselected ones are indicated with crosses.

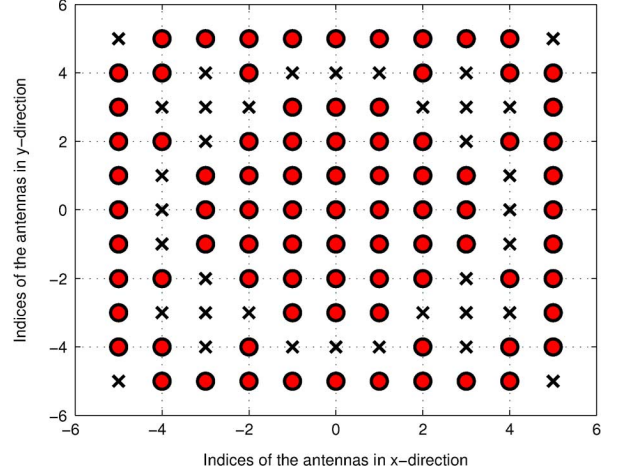


Fig. 6. 85 antennas selected by the proposed antenna selection method (9) in a  $11 \times 11$  array with original inter-element spacing of  $\lambda/2$ . Selected antennas are indicated with circles. Unselected antennas are indicated with crosses.

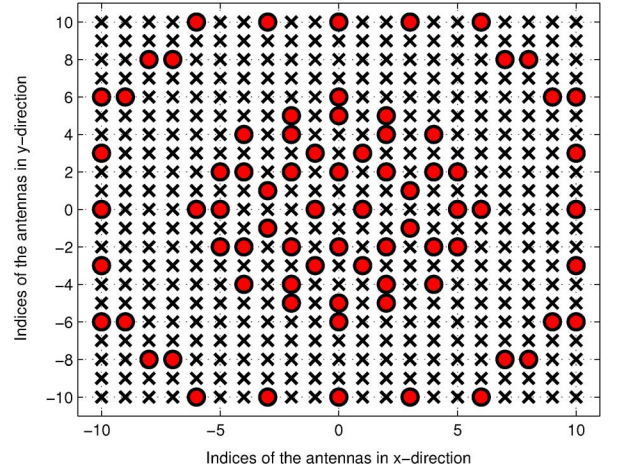


Fig. 7. 76 antennas selected by the proposed antenna selection method (9) in a  $21 \times 21$  array with original inter-element spacing of  $\lambda/4$ . Selected antennas are indicated with circles. Unselected antennas are indicated with crosses. This optimized array achieves the beam pattern in Fig. 8.

In the eighth example, the antenna selection method (9) is tested on a  $\lambda/4$  spaced array. Same specifications as the sixth example are used. To maintain the same aperture as the  $11 \times 11$  array, a  $21 \times 21$  array is used. The total number of antennas is 441. In the first iteration, a  $l_1$ -norm version of (9) is solved and the solution is 128 antennas. The final solution found by (9) is 76 antennas (obtained at the 4th iteration). The optimized array is shown in Fig. 7 with many inter-element spacings much greater than  $\lambda/2$ . Thus, sidelobe control is especially critical as grating lobes may appear. The resulting beam pattern in Fig. 8 still has its sidelobe level strictly maintained at  $-25.85$  dB. Only 63% of the antennas in the original  $11 \times 11$  array are selected by (9) in this example.

The antenna selection method (9) can reduce the DRR of  $\mathbf{w}$  ( $\text{DRR} = \max |w_i| / \min |w_i|$ ) by omitting elements with magnitudes ( $\leq \delta$ ). The DRRs of the beamforming weight vectors using (6) in the sixth example, as well as (9) in the seventh and eighth examples, are tabulated in Table I (same specifications are imposed in these examples). The antenna selection method

TABLE I  
DRRs OF BEAMFORMING WEIGHT VECTORS IN VARIOUS EXAMPLES

| Simulation example  | Number of selected antennas | DRR    |
|---|-----------------------------|--------|
| Example 6: Eq. (6) on $\lambda/2$ spaced $11 \times 11$ array | 121                         | 177.36 |
| Example 7: Eq. (9) on $\lambda/2$ spaced $11 \times 11$ array | 85                          | 33.27  |
| Example 8: Eq. (9) on $\lambda/4$ spaced $21 \times 21$ array | 76                          | 34.22  |

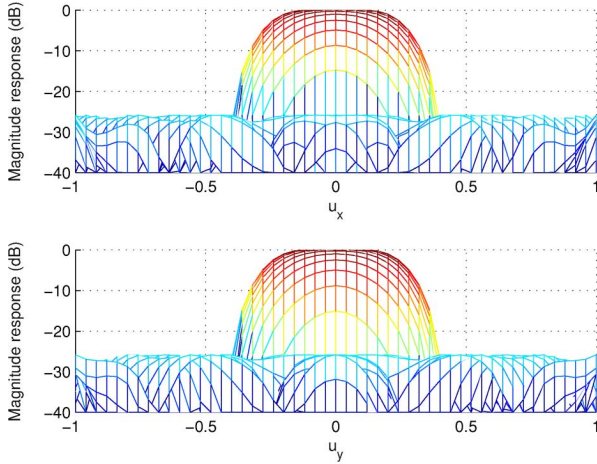


Fig. 8. Beam pattern with circular-shaped mainlobe and controlled sidelobe level achieved by the proposed antenna selection method (9) using 76 antennas. Top: View of beam pattern in  $u_x$  direction. Bottom: View of beam pattern in  $u_y$  direction.

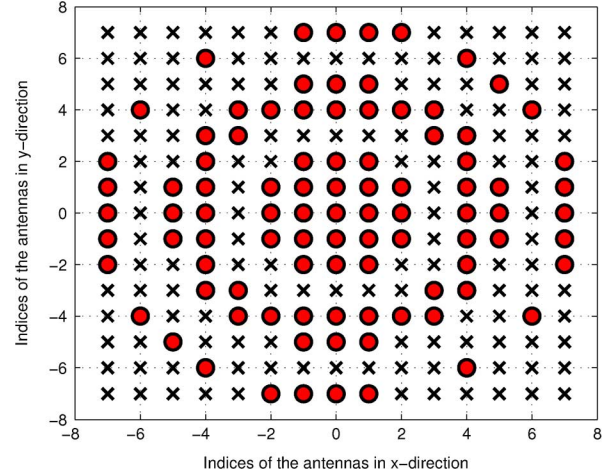


Fig. 10. 93 antennas selected by the proposed antenna selection method (9) in a  $15 \times 15$  array with original inter-element spacing of  $\lambda/2$ . Selected antennas are indicated with circles. Unselected antennas are indicated with crosses.

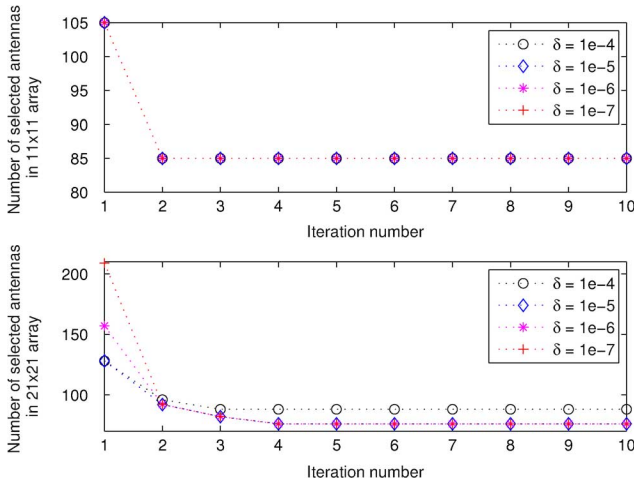


Fig. 9. Convergence of the proposed antenna selection method (9) at different  $\delta$  values, for the seventh and eighth examples. Top: Seventh example operates on the  $\lambda/2$  spaced  $11 \times 11$  array. Bottom: Eighth example operates on the  $\lambda/4$  spaced  $21 \times 21$  array.

(9) has lowered the DRRs of the beamforming weight vectors in the seventh and eighth examples compared to that obtained by the synthesis method (6) in the sixth example.

The choice of  $\delta$  in the antenna selection method (9) is discussed. A wide range of  $\delta$  values ( $10^{-4}$  to  $10^{-7}$ ) is tested, using the seventh ( $\lambda/2$  spaced  $11 \times 11$  array) and eighth ( $\lambda/4$  spaced  $21 \times 21$  array) examples. From Fig. 9, there is almost no difference in the final solution or the number of iterations needed to reach the final solution. The convergence of (9) is slower with

smaller  $\delta$  values. In the  $21 \times 21$  array example, (9) does not converge to the same final solution with  $\delta = 10^{-4}$  as with other  $\delta$  since elements in  $\mathbf{w}$  with magnitudes  $\leq 10^{-4}$  are considered unused, so more antennas are needed to meet the same specifications. To conclude, (9) is not very sensitive to the choice of  $\delta$  and  $\delta = 10^{-5}$  is found suitable for all the examples and they converge in a few iterations.

Finally, the antenna selection method (9) is used to design a non-uniformly spaced array for a circular-shaped mainlobe and controlled sidelobe level with specifications from [10]. The mainlobe region is  $u_x^2 + u_y^2 \leq 0.29^2$  with  $r_{dB} = 1$  dB and the sidelobe region is  $u_x^2 + u_y^2 \geq 0.44^2$  with  $\tau = -20$  dB. The method of [10] uses all the 100 antennas in a uniform  $\lambda/2$  spaced  $10 \times 10$  array. The antenna selection method (9) is tested on the same type of array and the result with the least number of selected antennas is reported. Only 93 antennas are selected by (9) (obtained at the 5th iteration) in a  $15 \times 15$  array to achieve the same specifications (beam pattern not shown for brevity). Compared to [10], (9) saves 7 antennas. The optimized array is shown in Fig. 10.

## VII. CONCLUSION

A convex optimization based beam pattern synthesis method with antenna selection has been proposed for linear and planar arrays. Thus, a sparse array requiring fewer antennas can be obtained that satisfies precisely the same beam pattern specifications achieved by a non-sparse array. This method can achieve a mainlobe of an arbitrary beamwidth and response ripple as well as completely arbitrary sidelobe levels. The

proposed method can design non-uniformly spaced arrays with inter-element spacings greater than one half-wavelength, without the appearance of grating lobes in the resulting beam-pattern. To compensate for undesirable effects in practice, robust beam-pattern constraints are derived. Simulations are conducted on arrays with up to a few hundred antennas to show the practicality of the proposed method.

## REFERENCES

- [1] A. B. Gershman, "Robust adaptive beamforming in sensor arrays," *AEU Int. J. Electron. and Commun.*, vol. 53, pp. 305–314, Jul. 1999.
- [2] S. A. Vorobyov, A. B. Gershman, and Z. Q. Luo, "Robust adaptive beamforming using worst-case performance optimization: A solution to the signal mismatch problem," *IEEE Trans. Signal Process.*, vol. 51, pp. 313–324, Feb. 2003.
- [3] J. Li, P. Stoica, and Z. Wang, "On robust Capon beamforming and diagonal loading," *IEEE Trans. Signal Process.*, vol. 51, pp. 1702–1715, Jul. 2003.
- [4] S. E. Nai, W. Ser, Z. L. Yu, and S. Rahardja, "A robust adaptive beamforming framework with beam-pattern shaping constraints," *IEEE Trans. Antennas Propag.*, vol. 57, pp. 2198–2203, Jul. 2009.
- [5] S.-P. Wu, S. P. Boyd, and L. Vandenbergh, "FIR filter design via spectral factorization and convex optimization," in *Appl. Computational Contr., Signal and Commun.*, B. N. Datta, Ed. Boston, MA: Birkhauser, 1997, vol. 1, pp. 215–245.
- [6] H. G. Hoang, H. D. Tuan, and B.-N. Vo, "Low-dimensional SDP formulation for large antenna array synthesis," *IEEE Trans. Antennas Propag.*, vol. 55, pp. 1716–1725, Jun. 2007.
- [7] S. E. Nai, W. Ser, Z. L. Yu, and S. Rahardja, "Beam-pattern synthesis with linear matrix inequalities using minimum array sensors," *Progr. Electromagn. Res. M*, vol. 9, pp. 165–176, 2009.
- [8] C. L. Dolph, "A current distribution for broadside arrays which optimizes the relationship between beam width and side-lobe level," *Proc. IRE*, vol. 34, pp. 335–348, Jun. 1946.
- [9] F.-I. Tseng and D. K. Cheng, "Optimum scannable planar arrays with an invariant sidelobe level," *Proc. IEEE*, vol. 56, pp. 1771–1778, Nov. 1968.
- [10] Y. U. Kim and R. S. Elliott, "Extensions of the Tseng-Cheng pattern synthesis technique," *J. Electromagn. Waves Appl.*, vol. 2, pp. 255–268, 1988.
- [11] P. M. Woodward and J. D. Lawson, "The theoretical precision with which an arbitrary radiation pattern may be obtained from a source of finite size," *J. Inst. Electr. Eng.*, vol. 95, pp. 363–370, Sep. 1948.
- [12] P. Y. Zhou and M. A. Ingram, "Pattern synthesis for arbitrary arrays using an adaptive array method," *IEEE Trans. Antennas Propag.*, vol. 47, pp. 862–869, May 1999.
- [13] Z. Shi and Z. Feng, "A new array pattern synthesis algorithm using the two-step least-squares method," *IEEE Signal Process. Lett.*, vol. 12, pp. 250–253, Mar. 2005.
- [14] C. A. Balanis, *Antenna Theory Analysis and Design*, 3rd ed. Hoboken, NJ: Wiley, 2005.
- [15] H. L. Van Trees, *Optimum Array Processing, Part IV of Detection, Estimation and Modulation Theory*. New York: Wiley, 2002.
- [16] J. F. Sturm, "Using SeDuMi 1.02, a MATLAB toolbox for optimization over symmetric cones," *Optimization Methods Softw.*, vol. 11–12, pp. 625–653, 1999.
- [17] S. P. Boyd and L. Vandenbergh, *Convex Optimization*. Cambridge, U.K.: Cambridge Univ. Press, 2004.
- [18] N. Karmarkar, "A new polynomial time algorithm for linear programming," *Combinatorica*, vol. 4, pp. 373–395, 1984.
- [19] J. A. Tropp, "Just relax: Convex programming methods for identifying sparse signals in noise," *IEEE Trans. Inf. Theory*, vol. 52, pp. 1030–1051, Mar. 2006.
- [20] E. J. Candès, M. B. Wakin, and S. P. Boyd, "Enhancing sparsity by reweighted  $l_1$  minimization," *J. Fourier Anal. Appl.*, vol. 14, pp. 877–905, Dec. 2008.
- [21] M. S. Lobo, M. Fazel, and S. P. Boyd, "Portfolio optimization with linear and fixed transaction costs," *Ann. Oper. Res.*, vol. 152, pp. 341–365, Jul. 2007.
- [22] H. Unz, "Linear arrays with arbitrarily distributed elements," *IRE Trans. Antennas Propag.*, vol. 8, pp. 222–223, Mar. 1960.
- [23] F. Wang, V. Balakrishnan, P. Y. Zhou, J. J. Chen, R. Yang, and C. Frank, "Optimal array pattern synthesis using semidefinite programming," *IEEE Trans. Signal Process.*, vol. 51, pp. 1172–1183, May 2003.



**Siew Eng Nai** (S'07) received the B.Eng. degree in electrical and electronic engineering from Nanyang Technological University (NTU), Singapore, in 2005, where she is currently working toward the Ph.D. degree.

From 2005 to 2006, she was employed as a Research Officer at the Institute for Infocomm Research (I<sup>2</sup>R), Agency for Science, Technology and Research (A\*STAR), Singapore. In 2010, she joined (I<sup>2</sup>R), (A\*STAR), as a Research Engineer. Her research interests include array signal processing.



**Wee Ser** (SM'97) received the B.Sc. (Hon) and Ph.D. degrees in electrical and electronic engineering from Loughborough University, U.K., in 1978 and 1982, respectively.

He joined the Defence Science Organization in 1982 and became Head of the Communications Research Division in 1993. In 1996, he was appointed the Technological Advisor to the CEO of the DSO National Laboratories. In 1997, he joined the Nanyang Technological University and has since been appointed Director of the Centre for Signal

Processing. He has published more than 120 research papers in refereed international journals and conferences. He holds six patents and is a coauthor of five book chapters. He is the Principal Investigator of several externally funded research projects. His research interests include sensor array signal processing, signal detection and classification techniques, and channel estimation and equalization.

Dr. Ser is currently an IEEE Distinguished Lecturer and an Associate Editor for *IEEE Communications Letters*, *Journal of Multidimensional Systems*, and *Signal Processing* (Springer). He is a member of a Technical Committee in the IEEE Circuit and System Society. He was a recipient of the Colombo Plan Scholarship and the PSC postgraduate scholarship. He was awarded the IEE Prize during his studies in the U.K. While in DSO, he was a recipient of the prestigious Defence Technology Prize (Individual) in 1991 and the DSO Excellent Award in 1992.



**Zhu Liang Yu** (S'02–M'06) received the B.S.E.E. and M.S.E.E. degrees in electronic engineering from the Nanjing University of Aeronautics and Astronautics, China, in 1995 and 1998, respectively, and the Ph.D. degree from Nanyang Technological University, Singapore, in 2006.

He worked as a Software Engineer at the Shanghai Bell Company, Ltd., from 1998 to 2000. In 2000, he joined the Centre for Signal Processing, Nanyang Technological University, as a Research Engineer, then became a Research Fellow. In 2008, he joined the College of Automation Science and Engineering, South China University of Technology, as an Associate Professor. His research interests include array signal processing, acoustic signal processing, and adaptive signal processing.



**Huawei Chen** (M'09) was born in Henan, China, in 1977. He received the B.S. degree from Henan Normal University, Xinxiang, China, in 1999 and the M.S. and Ph.D. degrees from Northwestern Polytechnical University, Xi'an, China, in 2002 and 2004, respectively.

In 2004, he joined the Department of Electronic Science and Engineering and the Institute of Acoustics, Nanjing University, China, as a Postdoctoral Researcher. From August 2005 to August 2009, he was with the Centre for Signal Processing, School of Electrical and Electronic Engineering, Nanyang Technological University, Singapore, as a Research Fellow. Since September 2009, he has been a Professor with the College of Information Science and Technology, Nanjing University of Aeronautics and Astronautics, China. His current research interests include array signal processing, acoustical and speech signal processing, and statistical and adaptive signal processing.